GEOPHYSICAL RESEARCH LETTERS, VOL. 39, L15501, doi:10.1029/2012GL052222, 2012

Minimum distribution of subsea ice-bearing permafrost on the U.S. Beaufort Sea continental shelf

Laura L. Brothers,[1] Patrick E. Hart,[2] and Carolyn D. Ruppel[1]

Received 2 May 2012; revised 25 June 2012; accepted 28 June 2012; published 7 August 2012.

[1] Starting in Late Pleistocene time (~19 ka), sea level rise inundated coastal zones worldwide. On some parts of the present-day circum-Arctic continental shelf, this led to flooding and thawing of formerly subaerial permafrost and probable dissociation of associated gas hydrates. Relict permafrost has never been systematically mapped along the 700-km-long U.S. Beaufort Sea continental shelf and is often assumed to extend to ~120 m water depth, the approximate amount of sea level rise since the Late Pleistocene. Here, 5,000 km of multichannel seismic (MCS) data acquired between 1977 and 1992 were examined for high-velocity (>2.3 km s^{-1}) refractions consistent with ice-bearing, coarse-grained sediments. Permafrost refractions were identified along <5% of the tracklines at depths of ~5 to 470 m below the seafloor. The resulting map reveals the minimum extent of subsea ice-bearing permafrost, which does not extend seaward of 30 km offshore or beyond the 20 m isobath.
Citation: Brothers, L. L., P. E. Hart, and C. D. Ruppel (2012), Minimum distribution of subsea ice-bearing permafrost on the U. S. Beaufort Sea continental shelf, *Geophys. Res. Lett.*, *39*, L15501, doi:10.1029/2012GL052222.

1. Introduction

[2] Since the Late Pleistocene, sea level rise of 120 m or more has flooded land that formerly lay at the edges of continents. In the circum-Arctic Ocean region, the now- flooded land consists of coastal plain sediments that in some areas had formerly developed continuous permafrost hundreds of meters thick while exposed subaerially during the extreme cold of Late Pleistocene time. Inundation of these coastal plain sediments has raised the average annual temperature at the former tundra surface by more than 15°C in some locations [*Taylor*, 1991]. This warming results in thawing of submerged permafrost and potential dissociation of methane hydrates that may have originally occurred in and beneath the permafrost [*Rachold et al.*, 2007]. Thawing permafrost is an important harbinger of climate change, but the possible release of methane from various sources (e.g., methane hydrates, remnant thermokarst lake thaw bulbs) on continental shelves has important implications for greenhouse warming [*Archer et al.*, 2009; *Ruppel*, 2011; *Shakhova et al.*, 2010b].

[3] Subsea permafrost degradation and associated methane emissions have been extensively studied on the East Siberian (Laptev Sea) margin, where the continental shelf extends hundreds of kilometers offshore [*Rachold et al.*, 2007]. Ocean water is supersaturated with methane in patches across the Laptev Sea shelf, possibly reflecting heterogeneous thawing of subsea permafrost and preferential release of methane from areas that are the most profoundly thawed [*Shakhova et al.*, 2010a]. In the Kara Sea, observations from high resolution seismic reflection data linked to coastal morphology have been used to map subsea permafrost [*Rekant et al.*, 2005]. On the Arctic margin of North America, detailed subsea permafrost mapping was completed in the Mackenzie Delta area of the Canadian Beaufort Sea over 25 years ago [*Hunter et al.*, 1978]. More recent studies there have focused on numerical modeling to predict the offshore extent of remaining methane hydrates [*Judge and Majorowicz*, 1992], documenting onshore occurrences of methane hydrate [*Dallimore and Collett*, 1995; *Dallimore et al.*, 2002], and characterizing seafloor methane emissions [*Paull et al.*, 2011].

[4] This paper focuses on the U.S. Beaufort Sea shelf, a 700 km section of the circum-Arctic Ocean region where the extent of subsea ice-bearing permafrost has never been fully mapped (Figure 1). Mapping ice-bearing permafrost gives a baseline for quantifying continued thawing of subsea permafrost during anticipated 21st century climate warming and provides insight about the impact of Late Pleistocene and Holocene warming and sea-level rise on methane release. The results also provide a basis for contrasting the subsea ice-bearing permafrost distribution on the U.S. Beaufort Sea shelf to that in other areas and for interpreting the differences in terms of varied geologic, glacial, and inundation histories. Finally, the subsea permafrost map yields important clues about the locations with the most potential for methane release due to dissociation of gas hydrates that may have been present in or beneath the flooded permafrost.

2. Setting

[5] The morphology of a continental shelf (e.g., width and steepness) affects the rate of inundation during sea level rise and the degree of warming experienced by underlying permafrost and possibly-associated gas hydrates. The U.S. Beaufort continental shelf ranges from 80 to 100 km wide from the shoreline to the 100 m isobath. Water depths are shallower than 20 m to distances of more than 20 km offshore, and seafloor relief is generally low except where ice-related processes have led to sediment scouring. Sediments defining the base of the Holocene section (~10 ka) are absent in much of the shallow U.S. Beaufort Sea, consistent with the final 40 m of sea level rise to present-day levels having occurred since 7.5 ka [*Hill et al.*, 1985]. Uncemented

[1]U.S. Geological Survey, Woods Hole, Massachusetts, USA.
[2]U.S. Geological Survey, Menlo Park, California, USA.

Corresponding author: L. L. Brothers, U.S. Geological Survey, 384 Woods Hole Rd., Woods Hole, MA 02543, USA. (lbrothers@usgs.gov)

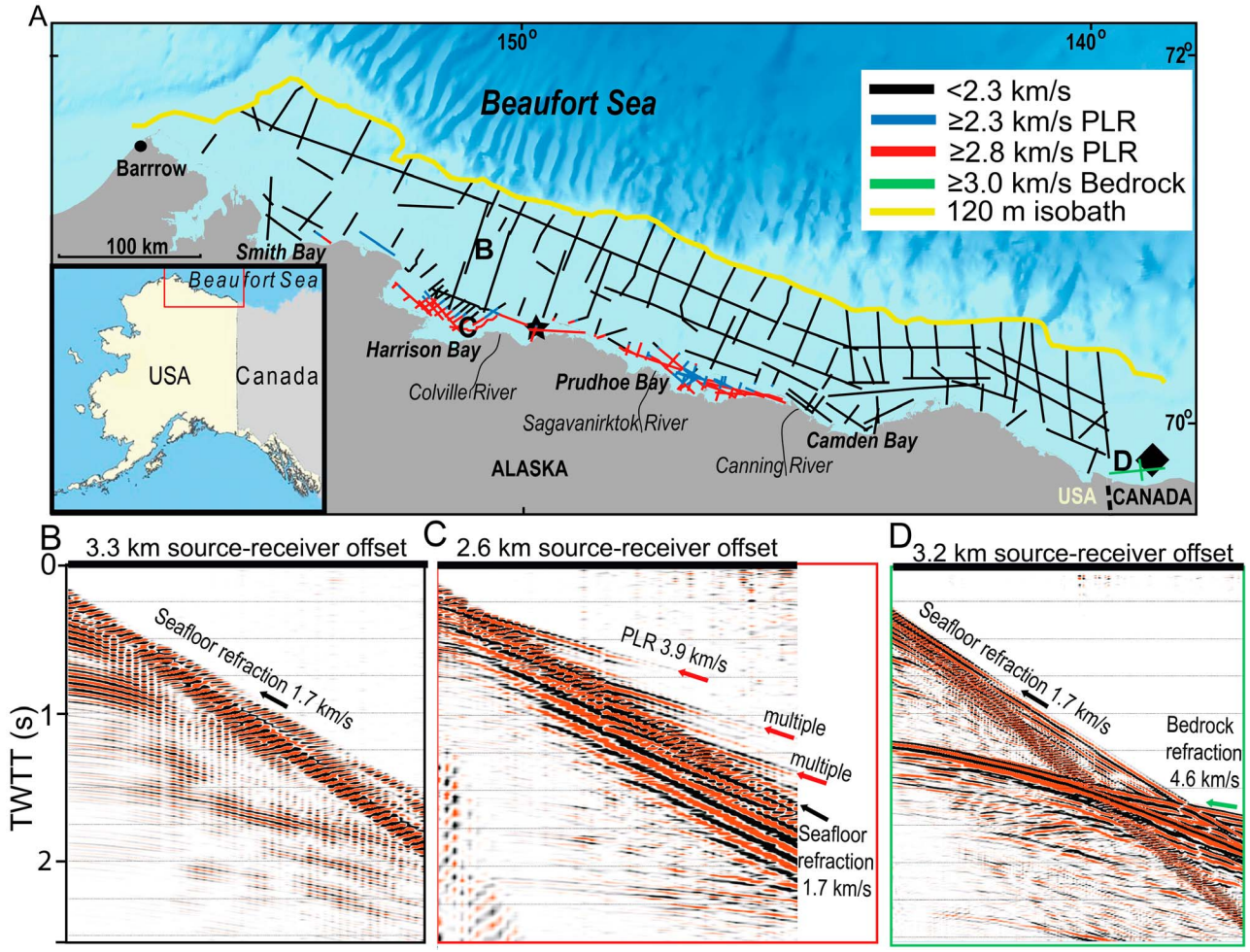

Figure 1. (a) Ice-bearing permafrost distribution on the U.S. Beaufort Sea shelf based on observation of high-velocity refractions (red, blue) in pre-stack seismic data with inset showing study location. The East Harrison Bay State well (star) intersects two examined transects and has permafrost at depths coincident with identified permafrost layer refractions (PLR) [*Collett et al.*, 1988]. The Edlok Well (diamond) identifies the mid-Eocene bedrock unconformity at depths where high velocity refractions occur on the eastern Beaufort shelf [*Dietrich and Lane*, 1992]. (b) The seismic record from a single shot is plotted with traces as a function of distance along the streamer. The y-axis is TWTT, and the slope of the first arrivals yields the velocity. This midshelf (22 m water depth) shot record lacks PLR and shows the refraction of near-seafloor sediments (black arrow). (c) Same as Figure 1b, but for a nearshore (5 m water depth) shot record that reveals a PLR and its two multiples (red arrows), which are distinct from the background seafloor refraction. (d) Same as Figure 1b, but for the eastern Beaufort (25 m water depth), revealing clear high velocity refraction (green arrow) associated with the mid-Eocene unconformity. The water column refraction ($\sim$1.5 km s^{-1}) intersects the right side of the panel at $\sim$2.4 s TWTT. This refraction crosses the seafloor and water refractions. Letters in Figure 1a denote shot record examples shown in Figures 1b, 1c, and 1d.

Tertiary and Quaternary sand, silt and clay make up the bulk of the shallow shelf sedimentary section, which has been deposited on older sediments [*Houseknecht and Bird*, 2011].

[6] The U.S. Beaufort continental shelf was not glaciated during the Late Pleistocene, and sustained subaerial exposure led to the development of ice-bearing permafrost hundreds of meters thick [*Lachenbruch et al.*, 1982]. Ice-bearing permafrost thicknesses onshore close to the present-day coastline range from 204 m in Barrow on the west to more than 660 m at Prudhoe Bay in the central U.S. Beaufort Sea sector [*Collett et al.*, 1988; *Jorgenson et al.*, 2008]. The pre-Holocene thickness of ice-bearing permafrost on the present-day continental shelf cannot be established, but the lateral extent of this permafrost on the shelf may have reached the 120 to 140 m isobath due to repeated sea level lowstands during the Pleistocene [*Bard and Fairbanks*, 1990; *Dinter et al.*, 1990].

[7] The top of the nominal stability zone for pure methane hydrate in areas of thick, continuous ice-bearing permafrost lies at $\sim$220 m depth and typically extends several hundred meters below the base of permafrost [e.g., *Ruppel*, 2011]. In our non-glaciated study area, we ignore the possibility of anomalously shallow gas hydrates (e.g., at depths of tens of meters) that some researchers argue could be leftover from the pressure effects of Late Pleistocene ice loading [*Chuvilin et al.*, 2000]. Gas hydrates on the North American Beaufort margin probably formed during the Pleistocene by in situ crystallization of abundant thermogenic gases migrating from conventional reservoirs, along with minor amounts of shallow microbial gas [*Collett et al.*, 1988]. Gas hydrate deposits

have been extensively described onshore between the Colville River and Sagavanirktok River in the Eileen and Tarn trends [*Collett*, 1993; *Collett et al.*, 2011] and may also occur in some other areas on the Alaskan North Slope [*Collett et al.*, 2008]. The ubiquity of intrapermafrost gas hydrate remains uncertain [*Dallimore and Collett*, 1995], but such gas hydrates certainly occur onshore within the study area [*Collett et al.*, 2011]. This observation is important since intrapermafrost gas hydrates, being more shallow, are more susceptible to long-term warming processes than those occurring beneath the base of permafrost [*Ruppel*, 2011].

[8] On the U.S. Beaufort margin, the best insights about the condition and distribution of ice-bearing permafrost and possible gas hydrate come from a limited number of offshore boreholes, seismic interpretations, and numerical modeling studies [*Herman*, 2011; *Osterkamp and Fei*, 1993]. These efforts have yielded sometimes contrasting interpretations of the seaward extent of permafrost owing both to the paucity of offshore observations [*Collett et al.*, 2011] and the difficulty of reconciling different types of observations. Most of the observational studies focus on shallow-water areas within ~5 km of the shoreline, with studies concentrated around Prudhoe Bay [*Morak and Rogers*, 1984], and offshore Barrow [*Osterkamp and Harrison*, 1982]. Until now, subsea ice-bearing permafrost has been mapped farther offshore only in Harrison Bay, a 1,100 km^2 area with maximum water depth of 10 m located just west of the Colville River Delta on the Central U.S. Beaufort Shelf [*Neave and Sellman*, 1984].

3. Methods

[9] This study relies on seismic velocity as the primary diagnostic for the presence of subsea ice-bearing permafrost. Laboratory and field studies indicate that the P-wave velocity (V_p) of ice-bearing coarse-grained sediments is strongly dependent on the saturation of ice in pore space. Using effective media theory and mixture models, *Johansen et al.* [2003] determine theoretical seismic velocities ranging from ~2.5 to 2.8 km s^{-1} for saturated sands with 0 to 40% ice saturation and from 3.4 km s^{-1} to as high as 4.35 km s^{-1} for ice filling 40 to 100% of pore space. The abrupt increase in seismic velocity at 40% saturation of the frozen pore-filling phase has also been observed in hydrate-bearing sediments [*Yun et al.*, 2007] and reflects the onset of cementation of sediment grains at this threshold saturation value. *Zimmerman and King* [1986] predict V_p of 2 to 2.4 km s^{-1} for 20% ice saturation in unconsolidated sediments with 50% and 30% porosity, respectively. *Rogers and Morack* [1980] measured velocities of 3 to 4 km s^{-1} in frozen sediments close to the shore in the Prudhoe Bay area.

[10] To assess the extent of subsea permafrost on the U.S. Beaufort Shelf, we analyzed ~5,000 km (~135,000 shot records) of prestack multichannel seismic (MCS) data acquired by industry and the U.S. Geological Survey (USGS) on the Beaufort Sea continental shelf between 1977 and 1992 (Figure 1a). The MCS surveys used airgun sources and produced shot records with 24 to 120 channels. Data quality varied between and along survey lines, and data collected in shallow, nearshore water depths (~3 m) had the worst signal-to-noise ratios.

[11] We used the seismic-refraction-velocity-based method described by *Hunter and Hobson* [1974] to map subsea ice-bearing permafrost between Barrow on the west and the Canadian border on the east. Using Focus and SeiSee software, data were first passed through a 12–48 Hz filter and then subjected to whole trace amplitude balancing. Each trace on an individual shot record was then plotted as a function of distance from the acoustic source with two-way travel time (TWTT) as the y-axis. Each shot record was examined for first-arrival refraction velocities (Figures 1b–1d). Independent velocity measurements made by coauthors on the same records varied no more than 5% (~0.1 km s^{-1}). Due to the acquisition technique, shot records are unreversed, and velocities are therefore not dip-corrected. Reflection data collected by the USGS in the nearshore of the Central U.S. Beaufort shelf 2010 and 2011 show that beds dip <1.5° northeast; thus, the effect of the dipping interfaces on the velocities determined by refraction analysis is negligible. Refraction depth was calculated using standard intercept-time methods, as applied to subsea ice-bearing permafrost by *Hunter et al.* [1978]. All data were combined in a GIS for spatial analysis.

4. Results

[12] Observed first arrival refraction velocities range from 1.7 to 4.6 km s^{-1} (Figure 1). Direct water velocity arrivals (~1.5 km s^{-1}) are not observed as first arrivals on these shot records because these data were acquired primarily in shallow water (<20 m). Seafloor refractions range from 1.7 to 2.1 km s^{-1} (Figure 1b). Of the 135,000 shot records examined, 37,000 have first arrival refractions with velocities ≥2.3 km s^{-1}. Ninety-six percent of the high velocity refractions occur nearshore along the central Beaufort shelf. Based on onshore and offshore well logs and related thermal mapping [*Collett*, 1993; *Lachenbruch et al.*, 1982], previous seismic surveys [*Neave and Sellman*, 1984; *Rogers and Morack*, 1980] and in-situ substrate velocity studies [*Morak and Rogers*, 1984], we interpret velocities ≥2.3 km s^{-1} as permafrost layer refractions (PLR) in that area (Figure 1c). On the eastern Beaufort shelf, we observe high velocity refractions with zero-offset intercept times of 1–1.5 s (>1000 m depth). This depth corresponds to the bedrock mid-Eocene unconformity identified in the Edlok well (Figure 1a) and mapped in reflection data by *Dietrich and Lane* [1992]. We therefore interpret these refractions as bedrock, not ice-bearing permafrost (Figures 1a and 1d).

[13] PLR occur in 26% of the examined shot point records on the shelf. The PLR are 5 to 470 m below the seafloor, deepen seaward, and have velocities ranging from 2.3 to 4.5 km s^{-1}. Sixty-seven percent of PLR have velocities of 2.8 km s^{-1} or greater. Measured PLR have a mean absolute depth of 195 m, with a standard deviation of 102 m. PLR occur on the central U.S. Beaufort shelf between the eastern side of Smith Bay and the western side of Camden Bay. The PLR extend nowhere more than 30 km offshore, nor beyond the 20 m isobath. The limited offshore extent of PLR is well-constrained and cannot be attributed to a paucity of data or to poor data quality. Numerous seismic lines cross from the PLR to no-PLR areas, and the boundary is well-delineated based on the seaward disappearance of the individual refractions. To provide further constraints, we focused on the relatively deep ice-bearing permafrost of Harrison Bay. Using stacked data,

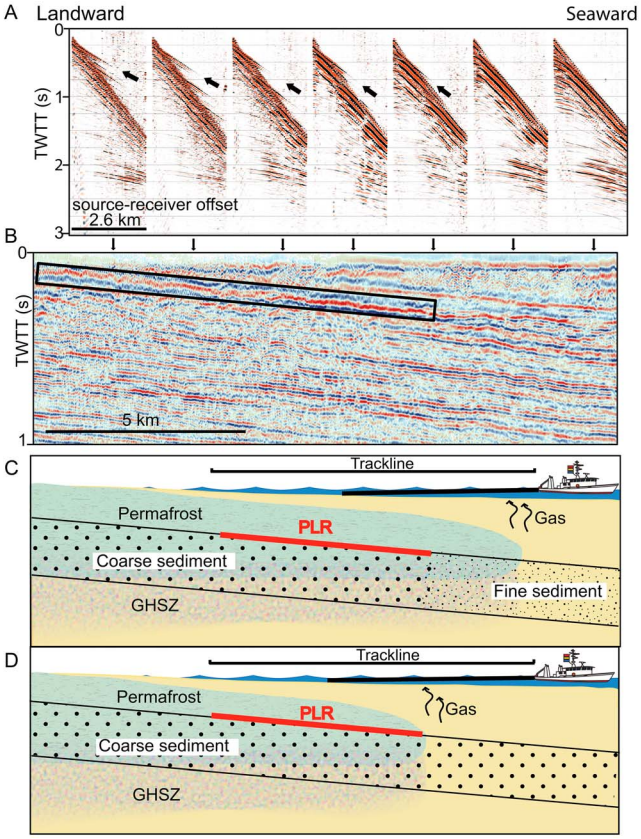

Figure 2. (a) A series of shot point records from Harrison Bay (line WB-314) shows an example of a PLR (arrows) abruptly terminating offshore. (b) In the line's poststack reflection data, PLR correspond to a stratigraphically-bound, high-amplitude, seaward-dipping reflection. Vertical arrows denote shot point records shown in Figure 2a. Conceptual models for the seaward termination of the PLR. (c) Abrupt seaward fining of offshore sediments in a dipping bed. In this case, subsea permafrost may truly extend beyond the apparent PLR termination that we map. (d) Illustration of the case in which the seaward termination of PLR marks the true seaward extent of contemporary subsea permafrost. Each model likely applies to parts of the U.S. Beaufort Sea margin. Dissociation of gas hydrates, if they exist, would be maximized near the seaward termination of subsea permafrost and is denoted by the black arrows, indicating methane escape.

we identified a high-amplitude reflection whose TWTT (0.1–0.3 s) and lateral extent correspond to the PLR identified in the pre-stack data (Figures 2a and 2b).

5. Discussion

[14] The velocity of the fine-grained frozen sediment is indistinguishable from some unfrozen sediments [*King et al.*, 1982; *Morak and Rogers*, 1984]. Thus, the reliance on seismic velocity to discriminate subsea ice-bearing permafrost from unfrozen sediments means that frozen fine-grained sediments may be missed in our analysis. At the same time, well logs and laboratory experiments indicate that fine-grained substrates are less likely than coarse-grained lithologies to host detectable ice [*Collett et al.*, 1988; *Zimmerman and King*, 1986]. Thus, frozen coarse-grained layers could be interbedded with seemingly unfrozen or low ice-content finer-grained layers even within a sedimentary section characterized by temperatures well below freezing.

[15] Our technique will only detect frozen coarse-grained layers, rendering the resulting map of subsea ice-bearing permafrost conservative: Subsea permafrost definitely occurs in the areas where we have identified PLR, but it may also occur in lithologies with significant fine-grained fractions on parts of the Beaufort shelf where we did not identify PLR (Figures 2c and 2d). Factors such as bed roughness and thickness also contribute to a substrate's propensity to form detectable high velocity refractions. Based on the quarter wavelength criteria, our method detects coarse-grained ice-bearing units >10 m thick. Seismic coverage of the shelf is not uniform, meaning that the map is likely biased by data coverage.

[16] The earliest studies of subsea ice-bearing permafrost interpreted high velocity refractions as the top of ice-bearing permafrost [*Hunter and Hobson*, 1974]. In other parts of the circum-Arctic Ocean, researchers continue to interpret a permafrost table (analogous to a groundwater table) from high-resolution seismic reflection data to represent the top of subsea ice-bearing permafrost [*Rekant et al.*, 2005]. A more nuanced interpretation of PLR-type features is reflected in later work by *Hunter et al.* [1978] and *Pullan et al.* [1987]. Like them, we emphasize that the refraction-based analysis method cannot definitively resolve the top of ice-bearing permafrost on the Beaufort Sea shelf. Fine-grained frozen sediments, which are undetectable due to lower seismic velocities, could, and likely do, reside above high velocity refractions, making resolution of the top of permafrost impossible.

[17] The distribution of PLR along the U.S. Beaufort shoreline corroborates the existence of laterally extensive ice-bearing strata in the greater Prudhoe Bay area and in Harrison Bay, two areas where researchers [*Neave and Sellman*, 1984; *Osterkamp et al.*, 1989] had previously detected subsea ice-bearing permafrost. The absence of PLR west of Smith Bay and east of the Canning River likely reflects the dominance of fine-grained lithologies such as siltstones and shales in these areas [*Collett et al.*, 1988; *Osterkamp and Payne*, 1981].

[18] PLR on the Central U.S. Beaufort shelf occur primarily within mostly sand-rich sedimentary deposits of the Sagavanirktok Formation [*Molenaar et al.*, 1986]. Based on depth, the few shallow PLRs (<60 m below the seafloor) are within the overlying Gubik Formation [*Craig and Thrasher*, 1982]. The sand-rich Sagavanirktok sediments host both ice and gas hydrates onshore, and the base of the formation's ice-bearing strata closely approximates the 0°C isotherm and is easily detected in well logs [*Collett*, 1993]. If these same sedimentary characteristics persist in the offshore continuation of the Sagavanirktok, then the abrupt seaward termination of PLRs within the coarse-grained layers of the formation most likely corresponds to the edge of ice-bearing permafrost (Figure 2d). Resistivity logs in one offshore well confirm that ice-bearing permafrost occurs at the same depth as the most proximal PLR (Figure 1a) [*Collett*, 1993].

[19] As noted above, the nominal maximum extent of subsea ice-bearing permafrost on circum-Arctic Ocean shelves is typically assumed to be the ~120 m isobath, based on the magnitude of global sea level rise since the Late Pleistocene. While well logs suggest that subsea ice-bearing permafrost and gas hydrates may be limited to the shelf area shallower

than the 50 m isobath [*Collett et al.*, 1988], our observations provide a more conservative interpretation of the distribution of subsea ice-bearing permafrost and show that it extends nowhere beyond the 20 m isobath. Ignoring subsidence, sedimentation, or erosion, the seafloor currently at the 20 m isobath has been inundated only since ~5 ka [*Hill et al.*, 1985], and pre-existing permafrost several hundreds of meters thick should still be thawing in these nearshore locations [*Pokrovsky*, 2003]. Whether the contemporary seaward extent of subsea ice-bearing permafrost is at the 20 or 50 m isobath, our findings imply that long-term warming associated with shelf flooding has likely produced enough thawing of subsea permafrost over the Holocene that the ice-bearing layers can no longer be detected seismically on the mid- and outer shelf. Such warming should also have led to the dissociation of any intrapermafrost gas hydrate and partial to full dissociation of subpermafrost gas hydrate [*Ruppel*, 2011] that might have been associated with the Late Pleistocene permafrost complex.

6. Conclusions

[20] Based on the analysis of pre-stack records of legacy seismic data, we have produced the first regional map of subsea ice-bearing permafrost on the U.S. Beaufort Sea continental shelf. Due to the reliance on seismic velocity to distinguish ice-bearing from ice-free layers, the map represents the minimal distribution of subsea ice-bearing permafrost, most likely in coarse-grained lithologies. The ice-bearing permafrost zone offshore is made up of individual, ice-bearing layers that are manifested as high-velocity PLR and intervening finer-grained lithologies whose ice content cannot be characterized by our approach. The interbedding of the PLR strata and other layers means that it is inappropriate to designate top of ice-bearing permafrost or a permafrost table on the shelf. The PLR end within 30 km of shore and do not extend beyond the 20 m isobath, implying that older assumptions about the present-day offshore extent of ice-bearing permafrost on this shelf should be revised to reflect the considerable thawing that has likely occurred since the onset of shelf inundation in the Late Pleistocene.

[21] **Acknowledgments.** This research was sponsored by DOE-USGS Interagency Agreement DE-FE0002911. L.B. was supported by a DOE NETL/NRC Methane Hydrate Fellowship under DE-FC26-05NT42248. We thank WesternGeco for the digital seismic data; N. Bangs, D. Brothers, T. Collett, P. Rekant, E. Rignot, W. Wood and an anonymous reviewer for constructive comments; and S. Dallimore, B. Herman, D. Houseknecht and V. Romanovsky for helpful discussions. Any use of trade names is for descriptive purposes and does not imply endorsement by the U.S. government.

[22] The Editor thanks Warren Wood and an anonymous reviewer for their assistance in evaluating this paper.

References

Archer, D., B. Buffett, and V. Brovkin (2009), Ocean methane hydrates as a slow tipping point in the global carbon cycle, *Proc. Natl. Acad. Sci. U. S. A.*, *106*(49), 20,596–20,601, doi:10.1073/pnas.0800885105.

Bard, H. B., and R. G. Fairbanks (1990), U-Th ages obtained by mass spectrometry in corals from Barbados: Sea level during the past 130,000 years, *Nature*, *346*, 456–458, doi:10.1038/346456a0.

Chuvilin, E. M., V. S. Yakushev, and E. V. Perlova (2000), Gas and possible gas hydrates in the permafrost of Bovanenkovo gas field, Yamal Peninsula, West Siberia, *Polarforschung*, *68*, 215–219.

Collett, T. S. (1993), Natural gas hydrates of the Prudhoe Bay and Kuparuk River area, North Slope, Alaska, *Am. Assoc. Pet. Geol. Bull.*, *77*(5), 793–812.

Collett, T. S., K. J. Bird, K. A. Kvenvolden, and L. B. Magoon (1988), Geologic interrelations relative to gas hydrates within the North Slope of Alaska, *U.S. Geol. Surv. Open File Rep.*, *88–389*, 150 pp.

Collett, T. S., W. F. Agena, M. W. Lee, M. V. Zyrianova, K. J. Bird, T. C. Charpentier, D. W. Houseknecht, T. R. Klett, R. M. Pollastro, and C. J. Schenk (2008), Assessment of gas hydrate resources on the North Slope, Alaska, *U.S. Geol. Surv. Fact Sheet*, *2008–3073*, 4 pp.

Collett, T. S., M. W. Lee, W. F. Agena, J. J. Miller, K. A. Lewis, M. V. Zyrianova, R. Boswell, and T. L. Inks (2011), Permafrost-associated natural gas hydrate occurrences on the Alaska North Slope, *Mar. Pet. Geol.*, *28*(2), 279–294, doi:10.1016/j.marpetgeo.2009.12.001.

Craig, J. D., and G. P. Thrasher (1982), Environmental geology of Harrison Bay, Alaska, *U.S. Geol. Surv. Open File Rep.*, *82–35*, 34 pp.

Dallimore, S. R., and T. S. Collett (1995), Intrapermafrost gas hydrates from a deep core hole in the Mackenzie Delta, Northwest Territories, Canada, *Geology*, *23*(6), 527–530, doi:10.1130/0091-7613(1995)023<0527:IGHFAD>2.3.CO;2.

Dallimore, S. R., T. S. Collett, T. Uchida, M. Weber, and H. Takahashi (2002), Overview of the 2002 Mallik Gas Hydrate Production Research Well Program, paper presented at 4th International Conference on Gas Hydrates, Takenaka Corp., Yokohama, Japan.

Dietrich, J. R., and L. S. Lane (1992), Geology and structural evolution of the demarcation subbasin and Herschel High Beaufort-Mackenzie Basin, Arctic Canada, *Bull. Can. Pet. Geol.*, *40*(3), 188–197.

Dinter, D. A., L. D. Carter, and J. Brigham-Grette (1990), Late Cenozoic geologic evolution of the Alaskan North Slope and adjacent continental shelves, in *The Geology of North America*, edited by A. Grantz, L. Johnson, and J. F. Sweeney, pp. 459–490, Geol. Soc. of Am., Boulder, Colo.

Herman, B. M. (2011), The distribution of permafrost beneath the Beaufort Sea Continental Shelf, Abstract C31A-0590 presented at 2011 Fall Meeting, AGU, San Francisco, Calif., 5–9 Dec.

Hill, P. R., P. J. Mudie, K. Moran, and S. M. Blasco (1985), A sea-level curve for the Canadian Beaufort Shelf, *Can. J. Earth Sci.*, *22*(10), 1383–1393, doi:10.1139/e85-146.

Houseknecht, D. W., and K. J. Bird (2011), Geology and petroleum potential of the rifted margins of the Canada Basin, in *Arctic Petroleum Geology*, *Geol. Soc. Mem.*, vol. 35, edited by A. M. Spencer et al., pp. 509–526, Geol. Soc., London.

Hunter, J. A., and G. D. Hobson (1974), Seismic refraction method of detecting sub-seabottom permafrost, in *The Coast and Shelf of the Beaufort Sea*, edited by J. C. Reed and J. E. Sater, pp. 401–415, Arct. Inst. of N. Am., San Francisco, Calif.

Hunter, J. A., K. G. Neave, H. A. MacAulay, and G. D. Hobson (1978), Interpretation of sub-seabottom permafrost in the Beaufort Sea, in *Third International Conference on Permafrost*, edited by C. B. Crawford, pp. 514–520, Natl. Res. Counc. of Can., Edmonton, Alberta, Canada.

Johansen, T. A., P. Digranes, M. van Schaack, and I. Lonne (2003), Seismic mapping and modeling of near-surface sediments in polar areas, *Geophysics*, *68*(2), 1–8.

Jorgenson, T., K. Yoshikawa, M. Kanevskiy, Y. Shur, V. Romanovsky, S. Marchenko, G. Grosse, J. Brown, and B. Jones (2008), Permafrost characteristics of Alaska, Institute of Northern Engineering, University of Alaska Fairbanks, 1 p.

Judge, A. S., and J. A. Majorowicz (1992), Geothermal conditions for gas hydrate stability in the Beaufort-Mackenzie area: the global change aspect, *Palaeogeogr. Palaeoclimatol. Palaeoecol.*, *98*(2–4), 251–263, doi:10.1016/0031-0182(92)90203-H.

King, M., B. Pandit, J. Hunter, and M. Gajtani (1982), Some seismic, electrical, and thermal properties of sub-seabottom permafrost from the Beaufort Sea, paper presented at 4th Canadian Conference on Permafrost, Natl. Res. Counc. of Can., Edmonton, Alberta, Canada.

Lachenbruch, A. H., J. H. Sass, B. V. Marshall, and T. H. J. Moses (1982), Permafrost, heat flow, and the geothermal regime at Prudhoe Bay, Alaska, *J. Geophys. Res.*, *87*(B11), 9301–9316, doi:10.1029/JB087iB11p09301.

Molenaar, C. M., K. J. Bird, and T. S. Collet (1986), Regional correlation sections across the North Slope of Alaska, *U.S. Geol. Surv. Misc. Field Stud. Map*, *MF 1907*.

Morak, J. L., and J. C. Rogers (1984), Acoustic velocities of nearshore materials in the Alaskan Beaufort and Chukchi Seas, in *The Alaskan Beaufort Sea: Ecosystems and Environments*, edited by P. W. Barnes, D. M. Schell, and E. Reimnitz, pp. 259–274, Academic, Orlando, Fla.

Neave, K. G., and P. V. Sellman (1984), Determining distribution patterns of ice-bonded permafrost in the U.S. Beaufort Sea from seismic data, in *The Alaskan Beaufort Sea: Ecosystems and Environments*, edited by P. W. Barnes, D. M. Schell, and E. Reimnitz, pp. 237–258, Academic, Orlando, Fla.

Osterkamp, T. E., and T. Fei (1993), Potential occurrence of permafrost and gas hydrates in the continental shelf near Lonely, Alaska, paper presented at 6th International Permafrost Conference, Chin. Soc. of Glaciol. and Geocryol., Beijing.

Osterkamp, T. E., and W. D. Harrison (1982), Temperature measurements in subsea permafrost off the coast of Alaska, paper presented at 4th Canadian Permafrost Conference, Natl. Res. Counc. of Can., Edmonton, Alberta, Canada.

Osterkamp, T. E., and M. W. Payne (1981), Estimates of permafrost thickness from well logs in northern Alaska, *Cold Reg. Sci. Technol.*, *5*, 13–27, doi:10.1016/0165-232X(81)90037-9.

Osterkamp, T. E., G. C. Baker, W. D. Harrison, and T. Matava (1989), Characteristics of the active layer and shallow subsea permafrost, *J. Geophys. Res.*, *94*(C11), 16,227–16,236, doi:10.1029/JC094iC11p16227.

Paull, C., et al. (2011), Tracking the decomposition of submarine permafrost and gas hydrate under the shelf and slope of the Beaufort Sea, paper presented at 7th International Conference on Gas Hydrates, Shell, Edinburgh, U. K.

Pokrovsky, S. I. (2003), Modeling permafrost and gas hydrate stability zones within Alaskan Arctic shelves and continental margins, PhD thesis, 136 pp., Univ. of Alaska Fairbanks, Fairbanks.

Pullan, S., H. A. Macaulay, J. A. M. Hunter, R. L. Good, R. M. Gagne, and R. A. Burns (1987), Permafrost distribution determined from seismic refraction, *Misc. Rep. 40*, 37 pp., Energy, Mines and Resour. Can., Whitehorse, Yukon, Canada.

Rachold, V., D. Y. Bolshiyanov, H.-W. Hubberton, R. Junker, V. V. Kunitsky, F. Merker, P. P. Overduin, and W. Schneider (2007), Nearshore Arctic subsea permafrost in transition, *Eos Trans. AGU*, *88*(13), 149, doi:10.1029/2007EO130001.

Rekant, P., G. Cherkashev, B. Vanstein, and P. Krinitsky (2005), Submarine permafrost in the nearshore zone of the southwestern Kara Sea, *Geo Mar. Lett.*, *25*(2–3), 183–189, doi:10.1007/s00367-004-0199-5.

Rogers, J., and J. Morack (1980), Geophysical evidence of shallow nearshore permafrost, Prudhoe Bay, Alaska, *J. Geophys. Res.*, *85*(B9), 4845–4853, doi:10.1029/JB085iB09p04845.

Ruppel, C. (2011), Methane hydrates and contemporary climate change, *Nat. Educ. Knowl.*, *2*(12), 12.

Shakhova, N., I. Semiletov, A. Salyuk, V. Yusupov, D. Kosmach, and O. Gustafsson (2010a), Extensive methane venting to the atmosphere from sediments of the East Siberian Arctic Shelf, *Science*, *327*(5970), 1246–1250, doi:10.1126/science.1182221.

Shakhova, N., I. Semiletov, I. Leifer, A. Salyuk, P. Rekant, and D. Kosmach (2010b), Geochemical and geophysical evidence of methane release over the East Siberian Arctic Shelf, *J. Geophys. Res.*, *115*, C08007, doi:10.1029/2009JC005602.

Taylor, A. E. (1991), Marine transgression, shoreline emergence: Evidence in seabed and terrestrial ground temperatures of changing relative sea levels, Arctic Canada, *J. Geophys. Res.*, *96*(B4), 6893–6909, doi:10.1029/91JB00293.

Yun, T. S., J. C. Santamarina, and C. Ruppel (2007), Mechanical properties of sand, silt, and clay containing tetrahydrofuran hydrate, *J. Geophys. Res.*, *112*, B04106, doi:10.1029/2006JB004484.

Zimmerman, R. W., and M. S. King (1986), The effect of the extent of freezing on seismic velocities in unconsolidated permafrost, *Geophysics*, *51*, 1285–1290.